

Kronecker-structured Sparse Vector Recovery with Application to IRS-MIMO Channel Estimation

Yanbin He and Geethu Joseph

Department of Microelectronics, Delft University of Technology, The Netherlands

Emails: {y.he-1,g.joseph}@tudelft.nl

Abstract—This paper studies the problem of Kronecker-structured sparse vector recovery from an underdetermined linear system with a Kronecker-structured dictionary. Such a problem arises in many real-world applications such as the sparse channel estimation of an intelligent reflecting surface-aided multiple-input multiple-output system. The prior art only exploits the Kronecker structure in the support of the sparse vector and solves the entire linear system together leading to high computational complexity. Instead, we break down the original sparse recovery problem into multiple independent sub-problems and solve them individually. We obtain the sparse vector as the Kronecker product of the individual solutions, retaining its structure in both support and nonzero entries. Our simulations demonstrate the superior performance of our methods in terms of accuracy and run time compared with the existing works, using synthetic data and the channel estimation application. We attribute the low run time to the reduced solution space due to the additional structure and improved accuracy to the denoising effect owing to the decomposition step.

Index Terms—Compressed sensing, basis expansion model, sparse Bayesian learning, Kronecker product, intelligent reflecting surface, singular value decomposition, angular sparsity

I. INTRODUCTION

Compressed sensing has been extensively applied in diverse domains, including data compression and sparse recovery [1]. Its success stems from the inherent redundancies of many real-world signals. With suitable bases, most information in such signals can be captured by a relatively small subset of bases and hence can be *sparsely* expressed over these bases [2]. Further, compressed sensing is a powerful tool for estimating the unknown parameters of non-linear functions by exploiting sparsity using the basis expansion model (BEM) [3]. Specifically, BEM expresses the parametric non-linear function as the product of a *known overcomplete dictionary* of the basis functions and a *unknown sparse coefficient vector*. Here, the basis functions of the non-linear function are obtained by sampling the unknown parameter over its range. As only a few functions corresponding to the ground truth are activated, the coefficient vector is sparse and can be recovered by solving the linear system using compressed sensing techniques.

Besides, BEM can exhibit more structures than simple sparsity, e.g., Kronecker-structured dictionary and Kronecker-structured support of the sparse vector, arising from image processing [4], [5] or wireless communications [6]–[9]. In general, such a problem takes the following canonical form,

$$\mathbf{y} = \mathbf{H}\mathbf{x} + \mathbf{n}, \quad (1)$$

where $\mathbf{y} \in \mathbb{C}^{\bar{M} \times 1}$ is the noisy measurement, $\mathbf{H} \in \mathbb{C}^{\bar{M} \times \bar{N}}$ is the dictionary with $\bar{M} < \bar{N}$, $\mathbf{x} \in \mathbb{C}^{\bar{N} \times 1}$ is the unknown sparse coefficient vector, and \mathbf{n} is the measurement noise. The Kronecker-structured dictionary can be represented as

$$\mathbf{H} = \otimes_{i=1}^I \mathbf{H}_i, \quad (2)$$

where $\mathbf{H}_i \in \mathbb{C}^{M_i \times N_i}$ with $\prod_{i=1}^I M_i = \bar{M}$ and $\prod_{i=1}^I N_i = \bar{N}$. Similarly, the support of \mathbf{x} can be expressed as the Kronecker product of I support vectors of sizes N_1, N_2, \dots, N_I . Here, the goal is to estimate \mathbf{x} given the Kronecker-structured dictionary \mathbf{H} and noisy measurement \mathbf{y} . The linear inversion problem (1) with Kronecker-structured dictionary (2) was widely discussed in literature [4]–[14]. A counterpart of the orthogonal matching pursuit (OMP), called Kronecker-OMP, matches the signal with the columns of different \mathbf{H}_i simultaneously [10]. However, this approach has low accuracy and requires hand-tuning of the stopping criterion. The problem (1) was also cast under the sparse Bayesian learning (SBL) framework in the previous studies, leading to a family of algorithms called Kronecker SBL (KroSBL) [7]–[9], [15]. SBL assumes a parameterized sparse-promoting prior distribution on \mathbf{x} , which can be flexibly manipulated to incorporate prior structural knowledge. These algorithms impose a zero mean fictitious Gaussian prior on \mathbf{x} to promote sparsity and exploit the Kronecker structure in \mathbf{x} by using the variance of \mathbf{x} as a Kronecker product of unknown hyperparameter vectors. This approach improved the recovery accuracy compared to Kronecker-OMP at the cost of higher computational complexity.

Furthermore, in applications like the intelligent reflecting surfaces (IRS)-aided wireless communication system, BEM can lead to a Kronecker-structured sparse vector, i.e., along with the support, the nonzero entries of \mathbf{x} are also Kronecker-structured [9]. For example, in the IRS channel estimation problem, BEM utilizes this angular sparsity by sampling pre-defined spatial angle grids for the angle-of-departure (AoD), angle-of-arrival (AoA), and the difference between the AoA and AoD and constituting the overcomplete dictionary with steering vectors of different combinations of the grid points. Then, different combinations of AoDs and AoAs result in the Kronecker-structured dictionary and sparse coefficients. Mathematically, the channel estimation takes the form of (1) and (2), and the sparse channel vector is given by

$$\mathbf{x} = \otimes_{i=1}^I \mathbf{x}_i, \quad (3)$$

where $\mathbf{x}_i \in \mathbb{C}^{N_i \times 1}$. Nonetheless, the existing algorithms [7]–[9], [11], [15] does not fully exploit the prior knowledge (3). Therefore, in this paper, we present an efficient method by enforcing (3) when searching for the solution to the linear inversion problem (1), with improved accuracy and run time compared to the state-of-the-art methods.

Our specific contributions are two-fold:

- *Algorithm*: Our method solves the linear inversion problem by first decomposing \mathbf{y} into I sub-vectors $\{\mathbf{y}_i\}_{i=1}^I$, obtaining each \mathbf{x}_i separately, and reconstruct the solution to (1) by Kronecker product of \mathbf{x}_i 's.
- *Numerical Results*: We numerically evaluate the performance of our method applied to the IRS-MIMO channel estimation problem. The results illustrate that our algorithm has low complexity (one-order less run time) and better accuracy compared to the benchmarking algorithms.

Overall, we explicitly integrate (3) into the sparse vector inference process to achieve better reconstruction performance and reduced computational time, making our algorithm a practical choice for IRS-MIMO channel estimation.

II. KRONECKER-STRUCTURED SPARSE VECTOR RECOVERY

We look at the Kronecker-structured sparse recovery problem of estimating the unknown vector \mathbf{x} from measurements \mathbf{y} given by (1) and the Kroncker-structured measurement matrix \mathbf{H} in (2). We also assume a Kronecker-structure for \mathbf{x} described by (3). In the following, we derive a decomposition-based algorithm to estimate the sparse vector \mathbf{x} .

To develop the algorithm, we start with the noiseless set of linear equations and extend to the noisy case later. Specifically, we begin with

$$\mathbf{y} = \mathbf{H}\mathbf{x}, \quad (4)$$

with $\mathbf{H} = \otimes_{i=1}^I \mathbf{H}_i$, and $\mathbf{x} = \otimes_{i=1}^I \mathbf{x}_i$. We next state a supporting lemma to devise a decomposition-based algorithm.

Lemma 1. [15, Lemma 4] *Consider a set of linear equations with $\mathbf{y}_1, \mathbf{y}_2 \neq \mathbf{0}$,*

$$(\mathbf{H}_1 \otimes \mathbf{H}_2)(\mathbf{x}_1 \otimes \mathbf{x}_2) = \mathbf{y}_1 \otimes \mathbf{y}_2. \quad (5)$$

Solving for \mathbf{x}_1 and \mathbf{x}_2 that satisfy (5) is equivalent to solving

$$\mathbf{H}_1 \mathbf{x}_1 = \alpha \mathbf{y}_1; \quad \mathbf{H}_2 \mathbf{x}_2 = \alpha^{-1} \mathbf{y}_2, \quad (6)$$

for any nonzero scalar α .

Lemma 1 can be trivially extended to the Kronecker product of I vectors, for any $I > 1$. So, Lemma 1 immediately suggests that the noiseless problem (4) can be decomposed into I smaller sparse recovery problems, instead of jointly solving for all the vectors $\{\mathbf{x}_i\}_{i=1}^I$. To elaborate, we can first decompose \mathbf{y} into $\{\mathbf{y}_i\}_{i=1}^I$ to disentangle different \mathbf{x}_i 's into I sub-problems, i.e., we find $\{\mathbf{y}_i \in \mathbb{C}^{M_i}\}_{i=1}^I$ such that $\mathbf{y} = \otimes_{i=1}^I \mathbf{y}_i$ and $\mathbf{y}_i = \mathbf{H}_i \mathbf{x}_i$. To find \mathbf{y}_i , we use the $(I-1)$ recursive rank-one decompositions, i.e., we solve for $\mathbf{y}_i \in \mathbb{C}^{M_i}$ such that for $i = 1, 2, \dots, I-1$,

$$\bar{\mathbf{y}}_{i-1} = \mathbf{y}_i \otimes \bar{\mathbf{y}}_i \quad \text{and} \quad \|\mathbf{y}_i\| = 1, \quad (7)$$

Algorithm 1 Decomposition-based sparse recovery

Input: Measurement \mathbf{y} , dictionaries \mathbf{H}_i for $i = 1, \dots, I$

Output: Sparse vector \mathbf{x}

- 1: **for** $i = 1, \dots, I$ **do**
 - 2: Solve (10) to obtain \mathbf{y}_i
 - 3: Solve (11) for \mathbf{x}_i using any compressed sensing algorithm
 - 4: **end for**
 - 5: Sparse vector $\mathbf{x} = \otimes_{i=1}^I \mathbf{x}_i$
-

where $\bar{\mathbf{y}}_0 = \mathbf{y}$ and $\bar{\mathbf{y}}_{I-1} = \mathbf{y}_I$. Further, since $\mathbf{y}_i \otimes \bar{\mathbf{y}}_i$ is the vectorized version of $\bar{\mathbf{y}}_i \mathbf{y}_i^T$, each *non-zero* row of $\bar{\mathbf{y}}_i \mathbf{y}_i^T$ can be a candidate for \mathbf{y}_i . Also, here we impose $\|\mathbf{y}_i\| = 1$ for $i = 1, \dots, I-1$ to avoid scaling ambiguity in \mathbf{y}_i , i.e., α in Lemma 1 is set to $\|\mathbf{y}_i\|^{-1}$ for $i = 1, \dots, I-1$. Once $\{\mathbf{y}_i\}_{i=1}^I$ is obtained, we solve I sparse recovery problems given by

$$\mathbf{y}_i = \mathbf{H}_i \mathbf{x}_i \quad \forall i = 1, 2, \dots, I, \quad (8)$$

to obtain $\{\mathbf{x}_i\}_{i=1}^I$ and the final estimate of $\mathbf{x} = \otimes_{i=1}^I \mathbf{x}_i$. We make two observations here. Firstly, the choice of scaling factor does not affect the final solution because of the Kronecker product. Secondly, due to the non-commutativity of the Kronecker product, the order of $\{\mathbf{y}_i\}_{i=1}^I$ automatically matches the order of $\{\mathbf{H}_i\}_{i=1}^I$, yielding (8).

In the noisy setting, the measurement decomposition step is

$$\arg \min_{\{\mathbf{y}_i \in \mathbb{C}^{M_i}\}_{i=1}^I} \|\mathbf{y} - \otimes_{i=1}^I \mathbf{y}_i\|_2, \quad (9)$$

and consequently, we replace (7) with $(I-1)$ rank-one approximations:

$$\mathbf{y}_i = \arg \min_{\mathbf{y}_i: \|\mathbf{y}_i\|_2=1, \bar{\mathbf{y}}_i \in \mathbb{C}^{\prod_{j=i+1}^I M_j}} \|\bar{\mathbf{y}}_{i-1} - \mathbf{y}_i \otimes \bar{\mathbf{y}}_i\|_2, \quad \forall i = 1, 2, \dots, I-1, \quad (10)$$

where $\bar{\mathbf{y}}_0 = \mathbf{y}$ and $\bar{\mathbf{y}}_{I-1} = \mathbf{y}_I$. The problem (10) can be solved recursively using singular value decomposition (SVD) or other rank-one approximation methods [16]. Then, we arrive at I separate sets of noisy linear equations:

$$\mathbf{y}_i = \mathbf{H}_i \mathbf{x}_i + \mathbf{n}_i, \quad \forall i = 1, \dots, I, \quad (11)$$

where \mathbf{n}_i is the noise term. We solve the above linear system using a standard sparse recovery algorithm such as OMP or SBL. The resulting algorithm, denoted as the decomposition-based Sparse Recovery (dSR), is summarized in Algorithm 1.

A. Complexity Analysis

The time and space complexities of Algorithm 1 are $\mathcal{O}(M^{I+1} + IT_{\text{CS}})$ and $\mathcal{O}(M^I + MN + S_{\text{CS}})$, respectively, assuming $M_i = M$, $N_i = N$, and $I \ll M < N$. Here, T_{CS} and S_{CS} are the time and space complexities of the sparse recovery algorithm used with dSR. Also, all sparse recovery sub-problems are independent of each other and can be solved in parallel. In that case, the time and space complexities dSR

TABLE I: Computation complexity of different SBL-based schemes.

Method	Time Complexity	Space Complexity
AM-KroSBL	$\mathcal{O}(R_{\text{EM}}(R_{\text{AM}}IN^I + (MN)^I))$	$\mathcal{O}((MN)^I)$
SVD-KroSBL	$\mathcal{O}(R_{\text{EM}}(N^{I+1} + (MN)^I))$	$\mathcal{O}((MN)^I)$
dSBL	$\mathcal{O}(R_{\text{EM}}N^2MI + M^{I+1})$	$\mathcal{O}(M^I + MN + N^2)$

changes to $\mathcal{O}(M^{I+1} + T_{\text{CS}})$ and $\mathcal{O}(M^I + IMN + IS_{\text{CS}})$, respectively.

As a concrete example, we consider dSR with SBL-based sparse recovery, namely decomposition-based SBL (dSBL). Table I provides a complexity comparison of dSBL and two other SBL-based algorithms from the family of KroSBL: alternating minimization-based KroSBL (AM-KroSBL) and SVD-KroSBL. Here, we denote the number of AM and EM iterations as R_{AM} and R_{EM} , respectively, and so for different SBL schemes, R_{EM} can be different. DSBL has better run time and memory requirements than KroSBL algorithms, and the difference is roughly of the order N^{I-1} .

B. Comparison with SVD-KroSBL

We start by noting that the family of KroSBL algorithms solves for a sparse vector with Kronecker-structured support, and does not assume a Kronecker structure on \mathbf{x} given by (3). KroSBL relies on Type-II learning to estimate the sparse vector \mathbf{x} , assuming that the measurement noise is Gaussian distributed, i.e., $\mathbf{n} \sim \mathcal{CN}(\mathbf{0}, \sigma^2 \mathbf{I})$. As discussed in Sec.I, it exploits the Kronecker-structured support of the sparse vector \mathbf{x} by using the following prior distribution on \mathbf{x} [9],

$$p(\mathbf{x}; \{\gamma_i\}_{i=1}^I) = \mathcal{CN}(\mathbf{0}, \text{diag}(\otimes_{i=1}^I \gamma_i)). \quad (12)$$

where $\{\gamma_i\}_{i=1}^I$ are the unknown hyperparameters. Then, KroSBL solves for $\{\gamma_i\}_{i=1}^I$ using the maximum-likelihood principle and uses this hyperparameter estimate to solve for \mathbf{x} . In particular, one version of KroSBL, called SVD-KroSBL, uses SVD in the r th iteration similar to our dSR as follows:

$$\gamma_i^{(r)} = \arg \min_{\gamma_i: \|\gamma_i\|_2=1, \bar{\gamma}_i \in \mathbb{R}^{N(I-i)}} \|\bar{\gamma}_{i-1} - \gamma_i \otimes \bar{\gamma}_i\|_2, \quad \forall i = 1, 2, \dots, I-1, \quad (13)$$

where $\bar{\gamma}_{I-1} = \gamma_I$ and $\bar{\gamma}_0 = \mathbf{d}$, which is function of the previous iterate $\{\gamma_i^{(r-1)}\}_{i=1}^I$. Clearly, (13) looks similar to our optimization problem (10). However, despite the akin form of (10) and (13), dSBL and SVD-KroSBL possess fundamental differences in the inference process. Firstly, the SVD-KroSBL adopts $\otimes_{i=1}^I \gamma_i$ to mimic the Kronecker structured support of the sparse vector (3), and not to decompose the original sparse recovery problem. Secondly, SVD-KroSBL is an iterative algorithm which upon convergence estimates the sparse vector \mathbf{x} is *jointly* using all $\{\gamma_i\}_{i=1}^I$ as given by [9, Eq. (18)]. This approach leads to a higher complexity as evident from Table I. Finally, the sparse structured $\gamma = \otimes_{i=1}^I \gamma_i$ does not ensure the Kronecker structure in the sparse vector \mathbf{x} modeled in (3). Similarly, if the assumption (3) does not hold, our dSR framework may fail. In short, the two algorithms lead to similar optimization problem formulation but are different

in their underlying principle and the nature of the final sparse vector estimate.

C. Denoising effect

As we show in Sec. IV, our dSR framework offers better reconstruction performance. One reason is that prior knowledge is directly incorporated into the inference process, as we have discussed before. Apart from this, our approach also holds the so-called *denoising effect* leading to a better performance. To see this, we reformulate (1) using the mixture property of the Kronecker product as

$$\mathbf{Y} = (\otimes_{i=2}^I \mathbf{H}_i \mathbf{x}_i) (\mathbf{H}_1 \mathbf{x}_1)^T + \mathbf{N} = \bar{\mathbf{y}}_1 \mathbf{y}_1^T + \mathbf{N}, \quad (14)$$

with $\text{vec}(\mathbf{Y}) = \mathbf{y}$, and $\text{vec}(\mathbf{N}) = \mathbf{n}$. We denote vectorization as operator $\text{vec}(\cdot)$. We notice that in the SVD step in (10) with $i = 1$, the goal is to recover a *rank-one* matrix estimate of $\bar{\mathbf{y}}_1 \mathbf{y}_1^T$ from measurements \mathbf{Y} deteriorated by a possibly *full rank* noise matrix \mathbf{N} . Therefore, solving the first step of (10) eliminates the noise power that is not in the span of the estimate of $\bar{\mathbf{y}}_1 \mathbf{y}_1^T$. So the noise the noise level reduces after the decomposition, which is called the denoising effect. We corroborate the idea using experimental results in Table II. The denoising effect helps our algorithm to achieve better reconstruction error, which is an added advantage apart from the shorter run time.

III. CASCADED CHANNEL ESTIMATION FOR AN IRS-AIDED SYSTEM

In this section, we discuss the application of our framework and algorithm to the problem of IRS-assisted MIMO channel estimation. For this, we consider an uplink narrowband millimeter-wave or terahertz band MIMO system with a T -antenna transmitter mobile station (MS) and an R -antenna receiver base station (BS), served by an L -element uniform linear array IRS. In the following, we present our system model using channel representation and transmission protocol.

We start with the channel model. As shown in Fig. 2, the IRS MIMO channel is the concatenation of the MS-IRS channel \mathbf{H}_{MS} and IRS-BS channel \mathbf{H}_{BS} . We model these channels using the Saleh-Valenzuela model [17] as

$$\mathbf{H}_{\text{MS}} = \sum_{p=1}^{P_{\text{MS}}} \sqrt{\frac{LT}{P_{\text{MS}}}} \beta_{\text{MS},p} \mathbf{a}_L(\phi_{\text{MS},p}) \mathbf{a}_T(\alpha_{\text{MS}})^H \in \mathbb{C}^{L \times T} \quad (15)$$

$$\mathbf{H}_{\text{BS}} = \sum_{p=1}^{P_{\text{BS}}} \sqrt{\frac{RL}{P_{\text{BS}}}} \beta_{\text{BS},p} \mathbf{a}_R(\alpha_{\text{BS},p}) \mathbf{a}_L(\phi_{\text{BS}})^H \in \mathbb{C}^{R \times L}, \quad (16)$$

where we define the steering vector $\mathbf{a}_Q(\psi) \in \mathbb{C}^{Q \times 1}$ for an integer Q and angle ψ with half-wavelength spacing as

$$\mathbf{a}_Q(\psi) = \frac{1}{\sqrt{Q}} \begin{bmatrix} 1 & e^{j\pi \cos \psi} & \dots & e^{j\pi(Q-1) \cos \psi} \end{bmatrix}^T. \quad (17)$$

Also, P_{MS} and P_{BS} are the number of spread angles, and we denote the p th AoA of the IRS, AoD of the MS, the p th

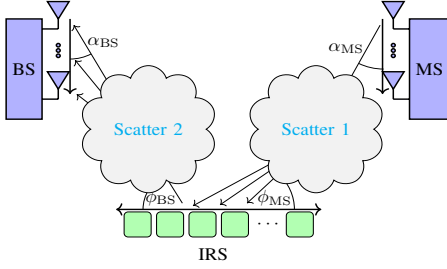


Fig. 1: An illustration of AoAs and AoDs in the uplink channel of an IRS-aided system [9].

AoA of the BS, and the AoD of the IRS as $\phi_{MS,p}$, α_{MS} , $\alpha_{BS,p}$, and ϕ_{BS} , respectively (see Fig. 1). For a given IRS configuration $\theta \in \mathbb{C}^{L \times 1}$, the cascaded MS-IRS-BS channel is then given by $\mathbf{H}_{BS} \text{diag}(\theta) \mathbf{H}_{MS}$. Here, the i th entry of θ represents the gain and phase shift due to the reflection of the i th IRS element. Then the object is to estimate the cascaded channel $\mathbf{H}_{BS} \text{diag}(\theta) \mathbf{H}_{MS}$ for any given IRS configuration θ .

Next, we look at the transmission protocol. We assume constant \mathbf{H}_{MS} and \mathbf{H}_{BS} over K coherent time slots. We send pilot data $\mathbf{X} \in \mathbb{C}^{T \times K_P}$ spanning K_P time slots repetitively for K_I IRS configurations $\{\theta_k\}_{k=1}^{K_I}$ such that $K = K_I K_P$. Then the received signal $\mathbf{Y}_k \in \mathbb{C}^{R \times K_P}$ corresponding to the k th configuration θ_k is

$$\mathbf{Y}_k = \mathbf{H}_{BS} \text{diag}(\theta_k) \mathbf{H}_{MS} \mathbf{X} + \mathbf{W}_k, \quad (18)$$

with $\mathbf{W}_k \in \mathbb{C}^{R \times K_P}$ being the zero-mean additive white Gaussian noise with variance σ^2 . To exploit the channel angular sparsity, we sample the angular domain at a set of N pre-defined grid angles $\{\psi_n\}_{n=1}^N$ with $\cos(\psi_n) = 2n/N - 1$ [18]. Then, we collect steering vectors of the grid angles to formulate the BEM dictionaries

$$\mathbf{A}_Q = [\mathbf{a}_Q(\psi_1) \quad \mathbf{a}_Q(\psi_2) \quad \dots \quad \mathbf{a}_Q(\psi_N)] \in \mathbb{C}^{Q \times N}, \quad (19)$$

for any integer $Q > 0$ referring to the number of elements in the array. Then the BEMs of (15) and (16) are

$$\mathbf{H}_{BS} = \mathbf{A}_R \mathbf{g}_R \mathbf{g}_{L,d}^H \mathbf{A}_L^H \text{ and } \mathbf{H}_{MS} = \mathbf{A}_L \mathbf{g}_{L,a} \mathbf{g}_T^H \mathbf{A}_T^H, \quad (20)$$

with $\mathbf{g}_R, \mathbf{g}_{L,d}, \mathbf{g}_{L,a}, \mathbf{g}_T \in \mathbb{C}^{N \times 1}$ carrying the unknown channel state information, including AoAs/AoDs of the channel and path gains. Rearranging (20) using (18) and reorganizing the received signal $\{\mathbf{Y}_k\}_{k=1}^{K_I}$ with some manipulations (see [9] for details), we arrive at

$$\tilde{\mathbf{y}} = (\Phi_L \otimes \Phi_T \otimes \Phi_R)(\mathbf{g}_L \otimes \mathbf{g}_T^* \otimes \mathbf{g}_R) + \tilde{\mathbf{w}} \in \mathbb{C}^{RK \times 1}, \quad (21)$$

where $\Phi_L \in \mathbb{C}^{K_I \times N}$ is formed by the first N columns of $\Theta^T (\mathbf{A}_L^T \odot \mathbf{A}_L^H)^T$, $\Phi_T = \mathbf{X}^T \mathbf{A}_T^*$, and $\Phi_R = \mathbf{A}_R$. Hence, (21) translates the channel estimation problem into a Kronecker-structured sparse recovery problem and we can apply Algorithm 1 to estimate the channel represented by $\mathbf{g}_L \otimes \mathbf{g}_T^* \otimes \mathbf{g}_R$.

IV. NUMERICAL EVALUTATION

In this section, we perform numerical simulations to evaluate the performance of dSR in two settings: sparse vector

recovery using synthetic data and IRS-aided communication channel estimation problem. We use two versions of dSR, namely decomposition-based OMP (dOMP) and dSBL where we use the standard OMP and SBL algorithms, respectively, in Step 3 of Algorithm 1. We implement classic SBL (cSBL) [19], orthogonal matching pursuit (OMP), AM-, and SVD-KroSBL [9] as benchmarks. Our code is available here.

A. Sparse Vector Recovery

For the linear system (1) with constraints (2) and (3), we set $I = 3$ and $N = 15$, resulting in $\mathbf{H} = \otimes_{i=1}^3 \mathbf{H}_i$ and $\mathbf{x} = \otimes_{i=1}^3 \mathbf{x}_i$ with $\mathbf{x}_i \in \mathbb{R}^{15 \times 1}$. The entries of $\mathbf{x}_i, \mathbf{H}_1 \in \mathbb{R}^{m \times 15}$, $\mathbf{H}_2 \in \mathbb{R}^{12 \times 15}$, and $\mathbf{H}_3 \in \mathbb{R}^{15 \times 15}$ are independently taken from $\mathcal{N}(0, 1)$. Here, m (referred to as measurement level) takes values from the set $\{2, 4, 6, 8, 10, 12, 14\}$, controlling the number of measurements $\bar{M} = 180m$ and the under-sampling ratio $\bar{M}/N^3 = 180m/3375$. Each \mathbf{x}_i has a sparsity level taking value from $S = \{2, 3, 4, 5, 6\}$, of which the support is drawn uniformly at random. We introduce zero-mean additive white Gaussian noise of which the power is determined by the signal-to-noise ratio $\text{SNR} (\text{dB}) = 10 \log_{10} \mathbb{E}\{\|\mathbf{H}\mathbf{x}\|_2^2 / \|\mathbf{n}\|_2^2\}$ from $\{5, 10, 15, 20, 25, 30\}$. Three metrics are considered for the performance evaluation: RMSE, support recovery rate (SRR), and run time. Here, we define

$$\text{RMSE} = \frac{\|\mathbf{x} - \hat{\mathbf{x}}\|_2}{\|\mathbf{x}\|_2} \text{ and } \text{SRR} = \frac{|\text{supp}(\hat{\mathbf{x}}) \cap \text{supp}(\mathbf{x})|}{|\text{supp}(\hat{\mathbf{x}}) \cup \text{supp}(\mathbf{x})|}, \quad (22)$$

where \mathbf{x} is the ground truth and $\hat{\mathbf{x}}$ is the estimated vector. We limit the number of iterations for the SBL-based methods (dSBL, cSBL, AM-KroSBL, and SVD-KroSBL) to a maximum of 150. In addition, we incorporate a pruning step to eliminate small hyperparameters as the EM algorithm unfolds [20], which can potentially expedite convergence. Our results, summarized in Fig. 2 and Tables II and III, are based on the average of 100 independent realizations.

The denoising effect is demonstrated in Table II. Here, we compare the noise levels of *i*) the original noisy signal \mathbf{y} in (1) and *ii*) the reconstructed signal $\hat{\mathbf{y}} := \otimes_{i=1}^3 \hat{\mathbf{y}}_i$ where $\hat{\mathbf{y}}_i$'s are the solution to the problem (10). It can be seen that the noise level reduces significantly after the decomposition, validating our claim on the denoising effect discussed in Sec. II-C. From Fig. 2 and Table III, we can see that with higher SNR, more measurements, and fewer non-zero entries, all algorithms, in general, yield RMSE and SRR, as expected. Our dSBL algorithm outperforms the other SBL-based algorithms and our dOMP outperforms the OMP algorithm, both in terms of RMSE, SRR, and run time. This observation demonstrates the efficacy of the decomposition idea. Compared to the SVD-KroSBL algorithm, dSBL has a slightly better support recovery rate because of the additional Kronecker structure accounted for by our dSBL algorithm. The relatively lower SRR performance of AM-KroSBL is due to its slow convergence, as pointed out in [15]. However, explicitly enforcing (3) leads to a notable difference in RMSE. Regarding dOMP, it only performs better than cSBL when SNR is low as in Fig. 2(a). With high SNR and sufficient measurements, dOMP is

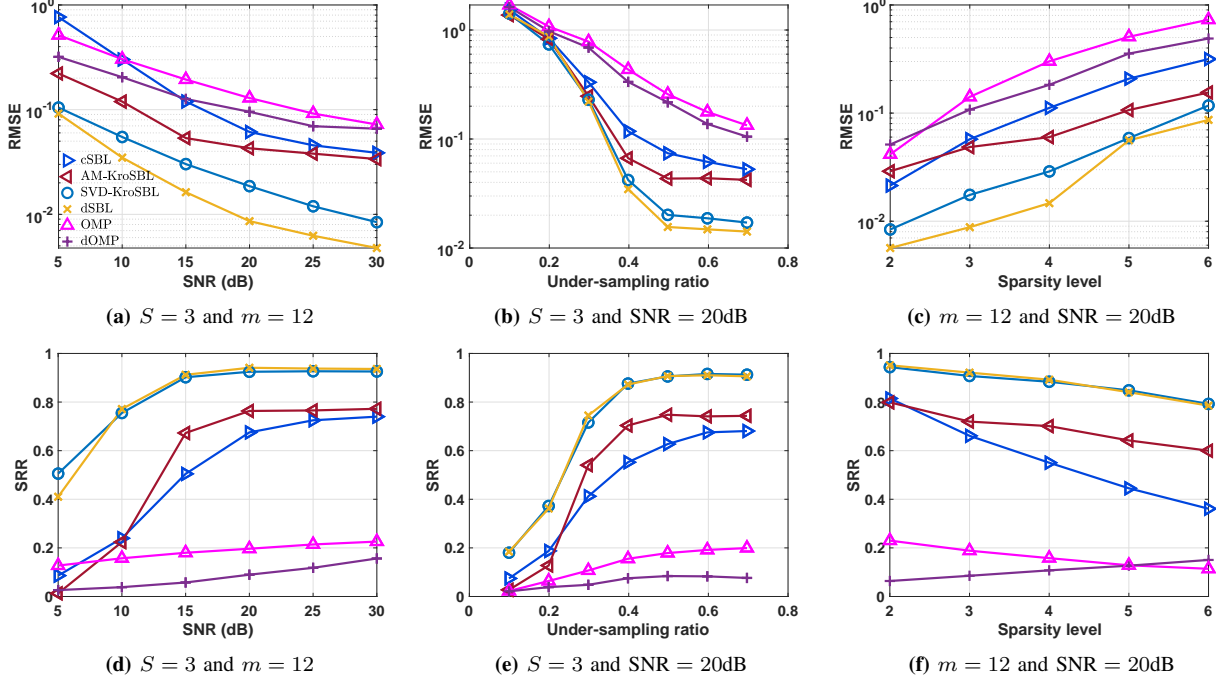


Fig. 2: RMSE and SRR performance of different algorithms as functions of SNR, under-sampling ratio, and sparsity level S . Unless otherwise mentioned in the plots, measurement level $m = 12$, sparsity level $S = 3$, and SNR = 20 dB.

TABLE II: Demonstration of denoising with $m = 12$, $S = 3$, using the original noisy signal \mathbf{y} , reconstructed signal $\hat{\mathbf{y}} = \otimes_{i=1}^3 \hat{\mathbf{y}}_i$ after the decomposition step, and ground truth \mathbf{y}_o .

SNR (dB)	5	10	15	20	25	30
$\ \mathbf{y} - \mathbf{y}_o\ $ (dB)	19.874	17.370	14.855	12.372	9.865	7.357
$\ \hat{\mathbf{y}} - \mathbf{y}_o\ $ (dB)	11.108	8.577	6.141	3.575	1.052	-1.507

TABLE III: Computation time of different schemes in sparse recovery. Here, the italics text represents the *best run time* and the underlined boldface text indicates the **second best run time**.

m	Time in seconds						
	2	4	6	8	10	12	14
cSBL	29.080	14.674	13.090	10.110	9.688	8.261	9.581
AM-KroSBL	5.829	4.049	4.656	4.814	6.357	8.234	7.959
SVD-KroSBL	2.675	1.570	2.356	1.255	1.070	1.256	1.208
dSBL	0.007	0.011	0.007	0.004	0.020	0.006	0.007
dOMP	0.003	0.002	0.003	0.003	0.004	0.004	0.003
OMP	0.115	0.207	0.190	0.301	0.348	0.460	0.406

incapable of outperforming other SBL-based algorithms but only its basic counterpart, i.e., OMP. So, due to its excellent performance, dSBL is a better choice over dOMP. Further, Table III indicates the low computational complexity of our dSR framework, corroborating our observation from Table I. It is interesting to note that dSBL is faster than the greedy method OMP.

B. Channel Estimation

In our IRS-assisted system simulation setup, we opt for $R = 16$ BS antennas, $T = 6$ MS antennas, $L = 256$ IRS elements, and $P_B = P_M = 3$. The IRS configuration entries

TABLE IV: Channel estimation time with different schemes. Here, the italics text represents the *best run time* and the underlined boldface text indicates the **second best run time**.

SNR (dB)	Time in seconds					
	5	10	15	20	25	30
cSBL	29.944	14.526	10.086	8.252	8.204	8.555
AM-KroSBL	26.745	7.510	4.859	4.045	4.452	6.826
SVD-KroSBL	13.764	3.677	2.440	2.322	1.287	1.869
dSBL	0.007	0.006	0.006	0.006	0.006	0.006
dOMP	0.002	0.002	0.001	0.001	0.001	0.001
OMP	0.083	0.085	0.081	0.084	0.083	0.085

$\{\theta_k\}_{k=1}^{K_I}$ are uniformly selected from $\{-1/\sqrt{N}, 1/\sqrt{N}\}$ with $K_I = 10$. We send $K_P = 4$ pilot signals for each IRS configuration, resulting in a total of $K = K_I K_P = 40$ pilot signals. We employ a pre-defined grid of $N = 18$ angles for constructing the BEM dictionaries, with all AoAs/AoDs assumed to be uniformly distributed on the grid for simplicity. The channel gains $\{\beta_{BS,p}\}_{p=1}^{P_B}$ and $\{\beta_{MS,p}\}_{p=1}^{P_M}$ in (15) and (16) are sampled from $\mathcal{CN}(0, 1)$ [21]. We use three performance metrics, i.e., RMSE, symbol error rate (SER), and run time for performance evaluation. Here, RMSE is given as

$$\frac{1}{K_I} \sum_{k=1}^{K_I} \frac{\|\mathbf{H}_{BS} \text{diag}(\theta_k) \mathbf{H}_{MS} - \tilde{\mathbf{H}}_{BS} \text{diag}(\theta_k) \tilde{\mathbf{H}}_{MS}\|_F}{\|\mathbf{H}_{BS} \text{diag}(\theta_k) \mathbf{H}_{MS}\|_F}, \quad (23)$$

with $\tilde{\mathbf{H}}_{BS} \text{diag}(\theta_k) \tilde{\mathbf{H}}_{MS}$ being the reconstructed channel. To compute the SER, we transmit 10^6 uncoded 8-QAM symbols through the actual channel. These symbols are then estimated using the reconstructed channel state information. We use 50

independent realizations of the channel, and the results, given in Fig. 3 and Table IV, are averaged across these trials.

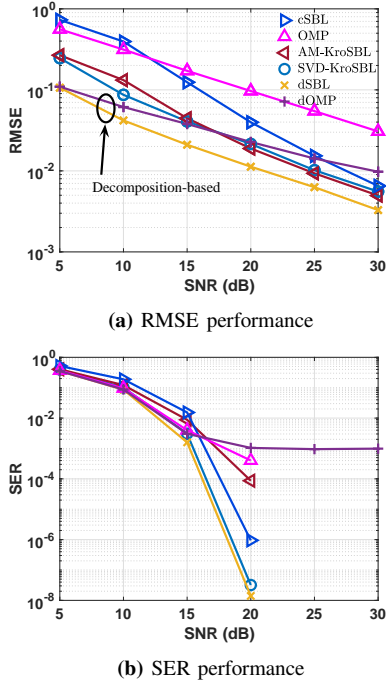


Fig. 3: RMSE and SER performance of different algorithms as functions of SNR with $K_I = 10$ and $K_P = 4$.

Here, we point out that the under-sampling ratio is $16 \times 40/18^3 \approx 10\%$, much lower than the results we showed in the previous section. Such a low measurement level is because the shorter coherent time for channel estimation and data transmission limits the number of pilot signals. The observations that we make about the synthetic data-based sparse recovery also hold in this case. Additionally, Fig. 3 and Table IV show that dSBL has the best performance in terms of RMSE, SER, and run time. Also, in the low SNR scenario, dOMP can outperform SBL-based methods other than dSBL. When SNR increases, dOMP still performs better than its non-decomposed counterpart OMP.

V. CONCLUSION

In this paper, we addressed the problem of sparse vector recovery with a Kronecker-structured dictionary and sparse vector. We explicitly incorporate the prior knowledge of the Kronecker structure into our solution by decomposing the problem into independent sub-problems. These problems are solved separately and the Kronecker product of the individual solutions gives the solution to the original problem. Our algorithm combines the best of both worlds by achieving better run time and accuracy than the existing algorithms because of dimensionality reduction and the denoising effect from decomposition. Our simulations demonstrate the effectiveness of our method for sparse recovery and channel estimation for an IRS-aided system. Establishing theoretical recovery guarantees for our approach and mathematically analyzing the denoising effect are interesting avenues for future research.

REFERENCES

- [1] Meenu Rani, Sanjay B Dhok, and Raghavendra B Deshmukh, "A systematic review of compressive sensing: Concepts, implementations and applications," *IEEE Access*, vol. 6, pp. 4875–4894, Jan. 2018.
- [2] Kenneth Kreutz-Delgado, Bhaskar Rao, Igor Fedorov, and Srinjoy Das, "Dictionaries in machine learning," in *Signal Process. Mach. Learn. Theory*, pp. 1073–1159. Elsevier, 2024.
- [3] Trevor Hastie, Robert Tibshirani, and Jerome Friedman, *The elements of statistical learning: data mining, inference, and prediction*, vol. 2, Springer, 2009.
- [4] Rongqiang Zhao, Qiang Wang, Jun Fu, and Luquan Ren, "Exploiting block-sparsity for hyperspectral Kronecker compressive sensing: A tensor-based Bayesian method," *IEEE Trans. Image Process.*, vol. 29, pp. 1654–1668, Oct. 2019.
- [5] Shuyuan Yang, Min Wang, Peng Li, Li Jin, Bin Wu, and Licheng Jiao, "Compressive hyperspectral imaging via sparse tensor and nonlinear compressed sensing," *IEEE Trans. Geosci. Remote Sens.*, vol. 53, no. 11, pp. 5943–5957, Jun. 2015.
- [6] Daniel Costa Araújo, Andre LF De Almeida, João PCL Da Costa, and Rafael T de Sousa, "Tensor-based channel estimation for massive MIMO-OFDM systems," *IEEE Access*, vol. 7, pp. 42133–42147, Mar. 2019.
- [7] Wen-Che Chang and Yu T Su, "Sparse Bayesian learning based tensor dictionary learning and signal recovery with application to MIMO channel estimation," *IEEE J. Sel. Top. Signal Process.*, vol. 15, no. 3, pp. 847–859, Apr. 2021.
- [8] Xiaowen Xu, Shun Zhang, Feifei Gao, and Jiangzhou Wang, "Sparse Bayesian learning based channel extrapolation for RIS assisted MIMO-OFDM," *IEEE Trans. Commun.*, vol. 70, no. 8, pp. 5498–5513, Aug. 2022.
- [9] Yanbin He and Geethu Joseph, "Structure-aware sparse Bayesian learning-based channel estimation for intelligent reflecting surface-aided MIMO," in *Proc. IEEE Int. Conf. Acoust., Speech, Signal, Process. (ICASSP)*, Jun. 2023, pp. 1–5.
- [10] Cesar F Caiafa and Andrzej Cichocki, "Block sparse representations of tensors using Kronecker bases," in *Proc. IEEE Int. Conf. Acoust., Speech, Signal, Process. (ICASSP)*, Mar. 2012, pp. 2709–2712.
- [11] Cesar F Caiafa and Andrzej Cichocki, "Computing sparse representations of multidimensional signals using Kronecker bases," *Neural Comput.*, vol. 25, no. 1, pp. 186–220, Jan. 2013.
- [12] Marco F Duarte and Richard G Baraniuk, "Kronecker product matrices for compressive sensing," in *Proc. IEEE Int. Conf. Acoust., Speech, Signal, Process. (ICASSP)*, Mar. 2010, pp. 3650–3653.
- [13] Marco F Duarte and Richard G Baraniuk, "Kronecker compressive sensing," *IEEE Trans. Image Process.*, vol. 21, no. 2, pp. 494–504, Aug. 2011.
- [14] Cesar F Caiafa and Andrzej Cichocki, "Multidimensional compressed sensing and their applications," *Wiley Interdiscip. Rev.: Data Min. Knowl. Discov.*, vol. 3, no. 6, pp. 355–380, Oct. 2013.
- [15] Yanbin He and Geethu Joseph, "Bayesian algorithms for Kronecker-structured sparse vector recovery with application to IRS-MIMO channel estimation," *arXiv preprint arXiv:2307.14719*, 2023.
- [16] Alyson K Fletcher and Sundeep Rangan, "Iterative reconstruction of rank-one matrices in noise," *Inf. Inference J. IMA.*, vol. 7, no. 3, pp. 531–562, 2018.
- [17] You You, Li Zhang, Minhua Yang, Yongming Huang, Xiaohu You, and Chuan Zhang, "Structured OMP for IRS-Assisted mmWave channel estimation by exploiting angular spread," *IEEE Trans. Veh. Technol.*, vol. 71, no. 4, pp. 4444–4448, Apr. 2022.
- [18] Zhendong Mao, Xiqing Liu, and Mugen Peng, "Channel estimation for intelligent reflecting surface assisted massive MIMO systems—A deep learning approach," *IEEE Commun. Lett.*, vol. 26, no. 4, pp. 798–802, Jan. 2022.
- [19] David P Wipf and Bhaskar D Rao, "Sparse Bayesian learning for basis selection," *IEEE Trans. Signal Process.*, vol. 52, no. 8, pp. 2153–2164, Aug. 2004.
- [20] Zhilin Zhang and Bhaskar D Rao, "Clarify some issues on the sparse Bayesian learning for sparse signal recovery," *University of California, San Diego, Tech. Rep.*, 2011.
- [21] Yuxing Lin, Shi Jin, Michail Matthaiou, and Xiaohu You, "Channel estimation and user localization for IRS-assisted MIMO-OFDM systems," *IEEE Trans. Wireless Commun.*, vol. 21, no. 4, pp. 2320–2335, Apr. 2021.